AIAA 2000-0914
Modeling Three-Dimensional Boundary Layers Using the Turbulent Potential Model

B. Perot and J. Taupier
University of Massachusetts
Amherst, MA

AIAA-2000-0914

MODELING THREE-DIMENSIONAL BOUNDARY LAYERS USING THE TURBULENT POTENTIAL MODEL

Blair Perot and Joris Taupier
Department of Mechanical & Industrial Engineering
University of Massachusetts
Amherst, MA 01003

ABSTRACT

Predictions of the three-dimensional turbulent boundary layer that results when two-dimensional channel flow is suddenly subjected to a spanwise pressure gradient are presented. The recently developed turbulent potential model is used to perform the calculations. The turbulent potential model demonstrates the ability to capture the initial decrease in turbulent kinetic energy and shear-stress, and accurately predicts the development of the spanwise velocity and resulting boundary layer skewing. Results are compared with direct numerical simulation data at a Reynolds number of 3300.

INTRODUCTION

Reynolds Averaged Navier-Stokes (RANS) turbulence models are usually concerned with modeling the Reynolds stress tensor. An alternative approach to RANS turbulence modeling has been proposed[1,2] where the primary modeled quantities are the scalar and vector potentials of the turbulent body force - the divergence of the Reynolds stress tensor. This approach has been found to have a number of attractive properties. The most important of which is the ability to model turbulence with the physical accuracy of Reynolds stress transport models but at a cost and complexity which is comparable to state-of-the-art k-ε models.

Like Reynolds stress transport equation models, the proposed model does not require a hypothesized constitutive relation between the turbulence and the mean flow variables. This allows non-equilibrium turbulence and complex three-dimensional flows to be modeled effectively. However, unlike Reynolds stress transport equation models, the proposed system of partial differential equations is much simpler to model and compute. It involves roughly half the number of variables, no realizability conditions, and removes the strong coupling between the equations. An analysis of the turbulent body force potentials and their physical significance[1] has revealed that they succinctly represent the relevant information contained in the Reynolds stress tensor and are fundamental turbulence quantities in their own right.

The most common modeling hypothesis relating the Reynolds stress tensor to the mean flow gradients is the eddy viscosity model, $\mathbf{R} = \frac{2}{3}k\mathbf{I} - \nu_T(\nabla\mathbf{u} + \nabla\mathbf{u}^T)$, where k is the turbulent kinetic energy and n_T is the eddy viscosity. More complex nonlinear extensions to the basic eddy viscosity hypothesis have been proposed[3-5] and these Algebraic Reynolds stress models fix a number of deficiencies in the standard linear eddy viscosity model. In particular, these nonlinear eddy viscosity models remove the restriction that the Reynolds stresses must be aligned with the mean flow gradients, which makes the representation of three-dimensional boundary layers theoretically possible. However, another common feature of three-dimensional boundary layers is that they are caused by significant changes in the flow geometry, and the turbulence is rarely allowed enough time to come into full equilibrium with the mean flow. Any algebraic constitutive equation between the mean flow and the Reynolds stresses, no matter how complex, relies on the assumption that turbulent equilibrium is present. Other turbulent flows of practical engineering significance which are not close to equilibrium include adverse pressure gradient boundary layers and rapidly strained flows. The equilibrium assumption imbedded in any constitutive relation for the Reynolds stress tensor is emphasized here because the proposed model avoids such a relation and therefore has the potential to predict non-equilibrium turbulent flows such as three-dimensional boundary layers more accurately.

There is some prior evidence that models which avoid a constitutive relation for the Reynolds stress tensor (and the associated equilibrium assumption) have the ability to outperform other models of the same general class. Both examples of this phenomenon come from models developed for nearly parallel shear flows (where the Reynolds shear stress is the important Reynolds stress). For example, the zero-equation model of Johnson & King[6] solves an ordinary differential equation for the maximum turbulent shear stress. As a result it often performs better than other zero-equation models which use the traditional approach of defining an eddy viscosity. A similar result is also obtained with one and two-equation models. The model of Bradshaw, Ferriss & Atwell[7] was widely accepted to be the most accurate model of the 1968 Stanford competition[8]. This model differed from the competitors in that it solved an equation for the shear stress directly, rather than using a constitutive equation involving the mean shear. The principal drawback of both these methods (and probably the reason that they are not more popular) is that they can only be applied to nearly parallel shear flows. In a very loose sense, the proposed model can be viewed as a way to generalize the modeling ideas of Bradshaw *et. al.* to arbitrary flows.

In the past, for arbitrary flows the only alternative to using a constitutive relation was to solve modeled transport equations for the Reynolds stress tensor itself. Reynolds stress transport models can potentially contain more physics than eddy-viscosity based models, however the equations are significantly more difficult to solve. In three-dimensions one must solve six highly coupled transport equations for each Reynolds stress. The equations are stiff, and none of the Reynolds stresses are universally dominant, so uncoupling the equations numerically is very difficult. In addition, the Reynolds stress tensor is a positive definite tensor but the modeled equations often do not preserve this property (realizability[9]). The turbulent potential model does not suffer from these difficulties. It involves half the equations of a Reynolds stress transport model. The equations are not strongly coupled and are not numerically stiff.

The key to developing a model which avoids the use of a constitutive relation and yet does not involve the complexity of a full Reynolds stress transport closure is to note that the Reynolds stresses contain more information than required by the mean flow. Only the divergence of the Reynolds stress tensor (a body force vector) is required to solve for the mean flow. With this in mind, the potential turbulence model defines two new turbulent quantities – the scalar and vector potentials of the body force vector. The advantages of a model that uses these turbulent potentials, rather than the body force vector itself, are twofold. Firstly, this allows the momentum equation to remain a conservative equation. Secondly, and more importantly, these potentials have a very clear physical interpretation which will facilitate the construction of models for their evolution. Turbulence modeling based on the force vector itself (or its rotational component – the Lamb vector) have been proposed by Wu, Zhou & Wu[10], and Marmanis[11], but the author is not aware of any model results based on these ideas.

TURBULENT POTENTIALS

The scalar potential, ϕ, and vector potential, y, of the turbulent body force are defined mathematically by the following equations.

$$\nabla\phi + \nabla \times y = \nabla \cdot \mathbf{R} \tag{1a}$$

$$\nabla \cdot y = 0 \tag{1b}$$

The second equation is a constraint on the vector potential. Other constraints are possible but this is the simplest for the purposes of our analysis. These equations can be rewritten to express the turbulent potentials individually.

$$\nabla^2\phi = \nabla \cdot (\nabla \cdot \mathbf{R}) \tag{2a}$$

$$\nabla^2 y = -\nabla \times (\nabla \cdot \mathbf{R}) \tag{2b}$$

The boundary conditions on these elliptic equations are constructed intuitively. Both potentials are required to go to zero at infinity, at a wall, or at a free surface. Note that by its very definition (Eqn. 1a) the scalar potential is the part of the turbulence that contributes to the mean pressure but does not effect the mean vorticity. Only the vector potential has the ability to effect the mean vorticity, and it only moves the vorticity around (enhanced transport), it does not create or destroy mean vorticity. Physically, we sometimes find it useful to regard the scalar potential as a measure of the average pressure drop in the cores of turbulent vortices, and the vector potential as a measure of the average vorticity magnitude of the turbulent vortices.

In flows with a single inhomogeneous direction (say the y-direction), Eqns. (2a) and (2b) simplify to $\phi = R_{22}$, $\psi_1 = -R_{23}, \psi_2 = 0, \psi_3 = R_{12}$. For this reason, it is also reasonable to view the vector potential as a conceptual generalization of the shear stress ($\overline{u'v'}$) to arbitrary geometries and three dimensions. In two-dimensional mean flows the vector potential is aligned perpendicular to the flow (like the vorticity) and has only a single nonzero component (ψ_3). The scalar potential (in combination with the turbulent kinetic energy) gives a good indication of the anisotropy of the turbulence and is fundamental to modeling the presence of walls and/or surfaces without using wall functions. The scalar potential is a positive semi-definite quantity in flows with a single inhomogeneous direction. It is hypothesized that this is also true for arbitrary flows.

In three-dimensional flows the presence of the divergence free constraint on the vector potential implies that the vector potential can be computed at a cost roughly equivalent to the scalar potential. Since the *k* and *e* transport equations are also solved with the model, the overall complexity and cost of solving the potential model is four transport equations in two-dimensions, and five transport equations in three-dimensions. This is only a slight reduction over the number of equations using in a full Reynolds stress transport equation closure (seven equations). However, the model has significant computational advantages because the equations are not as stiff as the Reynolds stress transport equations so they can be numerically uncoupled and solved as individual advection-diffusion equations.

TURBULENT POTENTIAL MODEL

The transport equations that constitute the turbulent potential model are summarized below.

$$\frac{Dk}{Dt} = \nabla \cdot (\nu + \nu_T / \sigma_k)\nabla k + P - \varepsilon \qquad (3a)$$

$$\frac{D\varepsilon}{Dt} = \nabla \cdot (\nu + \nu_T / \sigma_\varepsilon)\nabla \varepsilon + \beta \frac{\hat{\varepsilon}}{k}(C_{\varepsilon 1}P - C_{\varepsilon 2}\varepsilon + C_{\varepsilon 3}P_{3D}) \qquad (3b)$$

$$\begin{aligned}\frac{D\phi}{Dt} &= \nabla \cdot (\nu + \nu_T / \sigma_k)\nabla \phi \\ &- \left(2\alpha\frac{\hat{\varepsilon}}{k} + \frac{2\nu(\nabla\phi^{1/2}\cdot\nabla\phi^{1/2})}{\phi} + \frac{\varepsilon}{k}\frac{2}{(1+C_{p4}\frac{\nu_T}{\nu})}\right)\phi \\ &+ C_{p1}\frac{\varepsilon}{k}\frac{(1-\alpha)}{(1+25/Re)}(\tfrac{2}{3}k - \phi) + C_{p2}\frac{\phi}{k}P \\ &+ (C_{p2}+C_{p3})2\alpha\frac{\phi}{k}\left(\frac{\psi\cdot\psi}{\nu_T(1+25/Re)} - P\right)\end{aligned} \qquad (3c)$$

$$\begin{aligned}\frac{D\psi}{Dt} &= \nabla \cdot (\nu + \nu_T / \sigma_k)\nabla \psi \\ &- \left(\alpha\frac{\hat{\varepsilon}}{k} + \frac{2\nu(\nabla k^{1/2}\cdot\nabla\phi^{1/2})}{(k\phi)^{1/2}} + \frac{\varepsilon}{k}\frac{1}{(1+C_{p4}\frac{\nu_T}{\nu})}\right)\psi \\ &+ (1-C_{p2})\phi\omega - C_{p1}\frac{\varepsilon}{k}\frac{(1-\alpha)}{(1+25/Re)}\psi + C_{p2}\frac{\psi}{k}P \\ &+ (C_{p2}+C_{p3})2\alpha\frac{\psi}{k}\left(\frac{\psi\cdot\psi}{\nu_T(1+25/Re)} - P\right)\end{aligned} \qquad (3d)$$

where

$P = \psi\cdot\omega$, $P_{3D} = |w \times y|$, $\nu_T = C_\mu \dfrac{\phi k}{\varepsilon}$, $\hat{\varepsilon} = \varepsilon - 2\nu(\nabla k^{1/2})^2$, $\alpha = 1/(1+1.5\frac{\phi}{k})$, and $Re = k^2/(\nu\varepsilon)$.

And the constants are given by:

$\sigma_k = 0.8$, $\sigma_\varepsilon = 1.2$, $C_{e1} = 1.5$, $C_{e2} = 1.83$, $C_{\varepsilon 3} = C_{\varepsilon 1}$
$C_{p1} = 4.2$, $C_{p2} = \frac{3}{5}$, $C_{p3} = \frac{6}{7}$, $C_{p4} = .12$.

The two constants given by fractions are determined by matching Rapid Distortion Theory (RDT) in the case of strongly sheared turbulence. A detailed derivation of these equations is found in Perot[2].

Initially these equations appear daunting. In fact, they represent a fairly simple extension of the classic *k-e* equation system, and are relatively simple compared to Reynolds stress transport equation models. The second source term in the potential equations (in parentheses) is a dissipation-like term. This term is a standard dissipation model with two near-wall/surface modifications, one for the dissipation and one for the near wall pressure correlation term. These modifications are active in the laminar sublayer and allow the model to obtain the correct asymptotic behavior in the sublayer. The source terms involving the constants C_{p1} and C_{p2} are pressure-strain redistribution terms. The slow pressure-strain is based on return-to-isotropy and the fast pressure-strain is based on isotropization of the production model. The constants are set to common values for these models. The effects of system rotation and transition have been incorporated in earlier versions of the model but are not necessary in this context.

While the model includes transport equations for k and e it should be emphasized that the proposed model is a significant departure from standard two-equation models. k and e are now auxiliary quantities that are only used to help model the source terms in the turbulent potential evolution equations. They are not used to determine the Reynolds stress tensor or the resulting mean flow. The elimination of the constitutive equation for the Reynolds stresses is an important departure that removes one of the weaker modeling assumptions. A k-w implementation could easily be substituted for the current choice of k and e. If computational time is a serious issue, algebraic models for either or both of these variables can be used. In particular, for shear dominated flows such as boundary layers, $k = \frac{3}{2}(f + Ey \cdot y / f)$ and $\varepsilon = C_\mu P \frac{\phi k}{\psi \cdot \psi}$ are good approximations. The latter expression is equivalent to the linear eddy viscosity hypothesis. However, it is not used to model the mean flow, just the source terms in the evolution equations. Computations of turbulent channel flow with these algebraic expressions and $E = 1.1$ showed a reasonable agreement with the DNS data of Kim, Moin & Moser[12].

Some of the important theoretical properties of the model are summarized below:

- Correct decay of homogeneous isotropic turbulence.
- Correct behavior in the log layer.
- Correct behavior for homogeneous shear flows at early times or after the sudden introduction of mean shear along a streamline.
- Correct behavior for homogeneous shear flows at long times.
- Exact asymptotic behavior near walls.
- Exact asymptotic behavior at free surfaces.
- No functions of the wall normal distance.
- Stability/Numerical robustness (for the flows tested to date).
- Low Reynolds number implementation.
- Exact transport equations (albeit unclosed) from which to derive the model terms.
- No algebraic constitutive relations relating the turbulence to the mean flow.

THREE-DIMENSIONAL EFFECTS

The equations for k and e are the standard evolution equations for these quantities with the exception of the extra production term in the dissipation equation. This production term which appears in conjunction with the additional constant $C_{\varepsilon 3}$ is non-zero only in three-dimensional flows. In two dimensions both the vorticity and the vector potential point out of the two-dimensional plane. They are therefore always aligned and their cross product is zero. In a three-dimensional flow that is not in equilibrium, the vorticity will change direction and the vector potential will lag behind. The cross product therefore gives a measure of the degree of three-dimensionality in the flow. This concept could be used simply to quantitatively describe three-dimensional boundary layers, but here we use it to our advantage in the modeling of the dissipation evolution.

One important effect in three-dimensional boundary layers is the evolution of the underlying turbulent structures. For example, in the suddenly spanwise driven two-dimensional channel flow, the final state will be a new two-dimensional channel flow at an angle to the original flow and with a larger shear rate. However, the final state takes a long time to achieve, and the transient solution is actually the more interesting solution. When the two-dimensional channel flow feels the spanwise pressure gradient, the long near-wall streaks must turn. The streaks are the dominant near-wall structures in turbulent boundary layers. It is hypothesized that the streaks break up when they begin to turn and later reform into longer streaks. This breakup results in a smaller large-scale length scale for the turbulence. If we use the standard approximation for the turbulent length scale, $L = k^{3/2}/\varepsilon$, then this implies that the dissipation should increase and the turbulent kinetic energy should decrease when the streaks are disrupted.

The previous analysis suggests that the k/ε system (Eqn. 3a and 3b) should be modified to include three-dimensional effects. For channel flow, the production and dissipation terms in the k-equation are exact and can not be modified, we therefore look to modify the epsilon equation. Since the cross-product of the vorticity and the vector potential is a measure of the degree of three-dimensionality of the boundary layer, we assume that the streak disruption is proportional to the three-dimensionality. The three-dimensionality measure that is proposed has the units of production and a form very similar to the turbulent kinetic energy production. For channel flow, the dot product of the vorticity and the turbulent vector potential is an exact expression for the production of the turbulent kinetic energy. It is therefore, not unreasonable to include the cross-product of the vorticity and the turbulent vector potential in the production term for the dissipation. This has the effect of increasing the dissipation when strong three-dimensional effects are present. The increase in dissipation then causes the counterintuitive initial reduction in the turbulent kinetic energy and shear stresses that is observed in direct numerical simulations.

Durbin[13] has also modeled spanwise driven channel flow, and was the first to suggest that modifying the dissipation equation is the critical element of modeling three-dimensional boundary layers. It should be noted that in a standard k-ε models the vector potential and the vorticity are always aligned even in three-dimensional flows due to the linear eddy viscosity hypothesis, so the additional dissipation production term which is proposed here will be zero. It is critical to have a model for the turbulence which does not assume this type of alignment in order to capture three-dimensional boundary layers correctly.

SPANWISE DRIVEN CHANNEL FLOW

Spanwise driven channel flow at a mean flow Reynolds number of 3300 was studied by Moin *et. al.*[14] using direct numerical simulation (DNS). Durbin later modeled this flow with a Reynolds stress transport model. We now discuss the ability of the turbulent transport model to predict this type of strongly non-equilibrium three-dimensional boundary layer. As mentioned previously, in flows with a single inhomogeneous direction (such as channel flow), the turbulent body force potentials can be directly related to the Reynolds stresses. $\phi = R_{22}$, $\psi_1 = -R_{23}$, $\psi_3 = R_{12}$. This fact will be used to allow direct comparisons of the model predictions with the direct numerical simulation data for the Reynolds stresses.

The DNS data is for a channel flow where the suddenly applied spanwise pressure gradient is ten times the streamwise pressure gradient. The data is given at the time of the spanwise pressure gradient application (t=0) and at time increments of 0.3 thereafter up to a nondimensional time of 0.9. During this time the spanwise velocity increases rapidly and reaches the same order of magnitude of the streamwise velocity. However, nondimensional turbulent large eddy turn-over time is of the order of one, so it highly unlikely that the turbulence could be considered to be in equilibrium with the mean flow at any time during this simulation.

The mean streamwise velocity is shown in figure 1. The symbols are the DNS data and the solid lines are the model predictions. It is clear that neither the DNS data nor the predictions show any significant change in the streamwise velocity during this initial development of the flow.

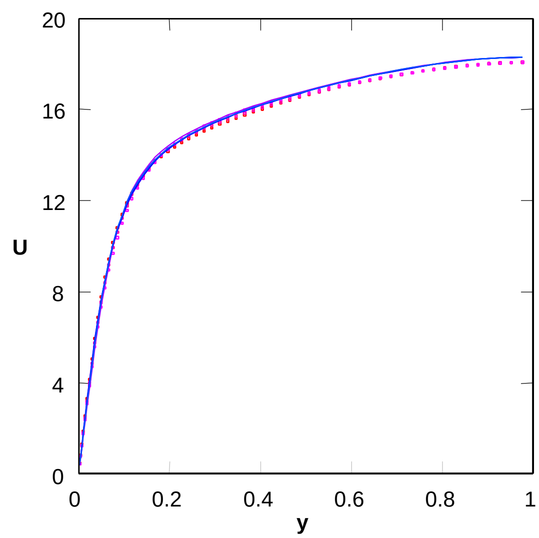

Figure 1. Streamwise mean velocity at times of 0.0, 0.3, 0.6 and 0.9 . Symbols are DNS data of Moin *et. al.*, solid lines are the turbulent potential model predictions

The mean spanwise velocity is shown in figure 2. The symbol convention remains the same in this and future graphs. Symbols are the DNS data of Moin *et. al.* and the solid lines are the turbulent potential model predictions. The mean spanwise velocity is roughly half the mean streamwise velocity at the final measurement time (t=0.9). The agreement with the DNS data is very good. But it is clear after comparing with the streamwise velocity profile, that the spanwise velocity profile is not yet a fully developed turbulent boundary layer profile. The turbulence has only just begun to effect the spanwise velocity profile at the final time. This good agreement of the spanwise velocity can be attributed to the non-equilibrium nature of the turbulent potential model. An equilibrium model, such as standard k/ε would apply the full turbulent eddy viscosity to the spanwise velocity immediately and cause the spanwise boundary layer to grow too rapidly.

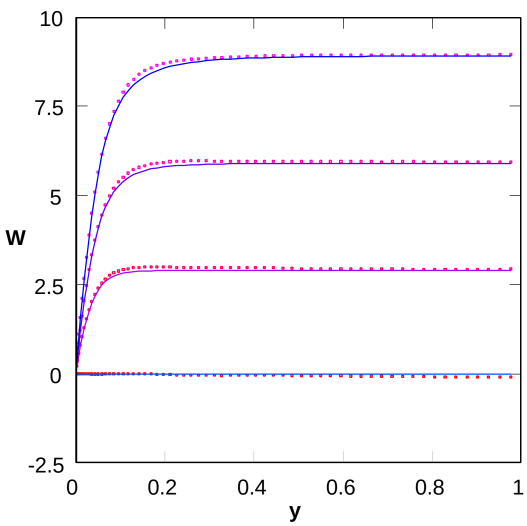

Figure 2. Spanwise mean velocity at times of 0.0, 0.3, 0.6 and 0.9 . Symbols are DNS data of Moin *et. al.*, solid lines are the turbulent potential model predictions

The evolution of the mean velocity profiles is further investigated by looking at the shear stresses. The $\overline{u'v'}$ and $\overline{u'w'}$ shear stresses are shown in figure 3. The upper set of curves are the $\overline{u'v'}$ shear stress. It is this stress which influences the evolution of the mean streamwise velocity. The DNS data is given by the symbols and the curves actually proceed from top to bottom as t=0.0, 0.3, 0.9, 0.6. The data is somewhat scarce but general picture for this shear stress is that initially it drops very slowly, between t=0.3 and t=0.6 it drops much more rapidly and then after that it begins to increase towards its initial value. The model predictions decrease monotonically, but display some of the same qualitative behaviors. The initial drop is very small, and speeds up at later times. While the predictions do not look very good, there appears to simply be a time delay in the predictions. Model predictions at a time t=1.2 (not shown) look very similar to the DNS data at t=0.6. We hope to eventually remove this time lag, but the mean flow predictions for the streamwise velocity show that, at least at these early times, that this defect is not fundamentally important.

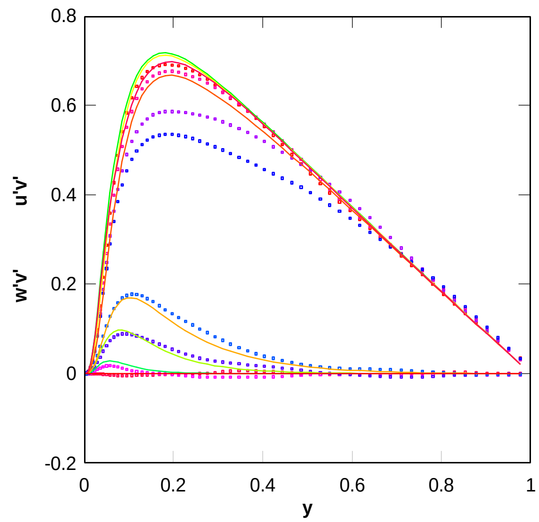

Figure 3. Turbulent shear stress profiles at times of 0.0, 0.3, 0.6 and 0.9 . Symbols are DNS data of Moin *et. al.*, solid lines are the turbulent potential model predictions. Upper group of curves are $\overline{u'v'}$, lower group of curves are $\overline{u'w'}$.

The lower group of curves in figure 3 are for the $\overline{u'w'}$ shear stress. The DNS data indicates that this stress starts at zero and increases monotonically as time proceeds. At very long times, this stress would be expected to be about ten times larger than the streamwise $\overline{u'v'}$ shear stress. However, at these early times it remains relatively small, approaching 25% of the $\overline{u'v'}$ shear stress at the final time (t=0.9). The turbulent potential model predictions (solid lines) closely match the DNS at these early times.

The normal stress $\overline{v'v'}$ is shown in figure 4. The normal stress does not directly affect the mean flow predictions as the shear stresses do, but it is important in predictions of heat transfer, and scalar transport in boundary layers. The DNS data indicates that at very early times the normal stress decreases extremely slowly. The data for time t=0 and time t=0.3 are on top of each other. After this the normal stress decreases slowly with time. This is thought to be a result of the disruption of the near wall streaks into shorter streaky structures and the enhanced dissipation that these shorter structures produce. It takes some time for the streaks to break up, and the dissipation to increase. The model predictions show roughly the same qualitative behavior. The initial decrease in the shear stress is very slow, and accelerates as time proceeds. As with the $\overline{u'v'}$ shear stress, the normal stress does not drop as quickly as the DNS results. This is again attributed to be due to the fact that the model lags the DNS data in time.

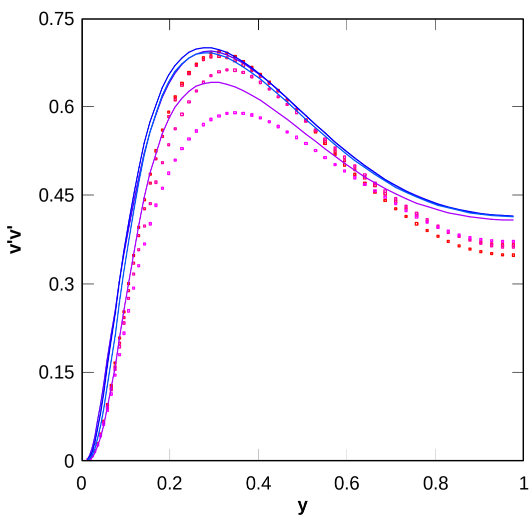

Figure 4. Normal stress, $\overline{v'v'}$, profiles at times of 0.0, 0.3, 0.6 and 0.9 . Symbols are DNS data of Moin *et. al.*, solid lines are the turbulent potential model predictions.

The turbulent kinetic energy profiles are shown in figure 5. The DNS data shows the turbulent kinetic energy decreasing in magnitude as time proceeds. However, it should be noted that the decrease occurs very slowly at first, rapidly between time t=0.3 and time t=0.6, and then slowly again after that time. It is hypothesized that the turbulent kinetic energy magnitude will begin to increase soon after t=0.9, in response to the ever increasing mean shear and turbulence production. At this very low Reynolds number, the model predictions for the turbulent kinetic energy are in considerable error even for the two-dimensional channel flow at time t=0. For two-dimensional channel flow Reynolds numbers of 7500 and 11,000 the model shows much better agreement of the turbulent kinetic energy with DNS data. Despite, the inaccuracy of the initial turbulent kinetic energy profile, the turbulent potential model shows the correct qualitative behavior in time. Proceeding from top to bottom the curves are at time 0.0, 0.3, 0.9, 0.6. So the turbulent kinetic energy actually drops to roughly the correct value at t=0.6 and then begins to increase after that time.

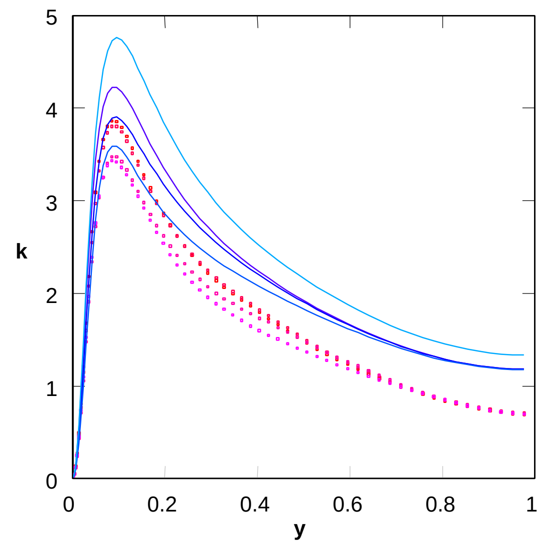

Figure 5. Turbulent kinetic energy profiles at times of 0.0, 0.3, 0.6 and 0.9 . Symbols are DNS data of Moin *et. al.*, solid lines are the turbulent potential model predictions.

One important aspect of the turbulent potential model is that, unlike the standard two equation models, the accuracy of the turbulent kinetic energy has very little impact on the over accuracy of the mean flow predictions. This is because k does not appear in the mean flow evolution equation. It only appears in the modeling of the source terms in the turbulent potential evolution equations.

CONCLUSIONS

The turbulent potential model demonstrates the ability to accurately predict the mean flow behavior of the suddenly spanwise driven channel flow at early times. The turbulence quantities show a reasonable agreement with the data and the correct qualitative trends both spatially and temporally.

While the geometry of this unsteady three-dimensional boundary layer is very simple, its behavior, particularly at these early times, is complex. The turbulence is not in equilibrium with the rapidly changing mean flow. In addition to the well known skewing of the boundary layer as one moves away from the wall, the turbulence quantities display a counterintuitive magnitude drop even while the overall magnitude of the mean shear increases.

It is thought that the spanwise velocity profile and the resulting boundary layer skewing are well captured because the turbulent potential model is a non-equilibrium model. The lack of a constitutive equation between the mean flow and the Reynolds stress tensor, allows the spanwise shear stress, $\overline{w'v'}$, to develop slowly in time, rather than instantly appearing along with the spanwise shear.

The drop in the turbulence quantities at early times is explained physically as a disruption of the long streaks in the near wall region into shorter structures. This disruption mechanism is modeled as an extra production term in the dissipation equation. This extra term is zero in two-dimensional flows and its magnitude is proportional to the degree of three-dimensionality in three-dimensional flows. Finally, this extra term has a mathematical form that is closely related to the turbulent kinetic energy production term and is therefore aesthetically pleasing on modeling grounds.

ACKNOWLEDGEMENTS

This work was funded by the Office of Naval Research, Grant number N00014-99-1-0194. Their support is gratefully acknowledged.

REFERENCES

1. B. Perot & P. Moin, "A new approach to turbulence modeling", Proceedings of the 1996 CTR Summer Program, Center for Turbulence Research, Stanford University/NASA Ames, 35-46 (1996).
2. B. Perot, "Turbulence modeling using body force potentials", Phys. Fluids, **11** (9), 2645-2656, (1999).
3. W. Rodi, "A new algebraic relation for calculating the Reynolds stresses", ZAMM **56**, 219-221 (1976).
4. S. B. Pope, "A more general effective-viscosity hypothesis", J. Fluid Mech. **72**, 331-340 (1975).
5. T. B. Gatski & C. G. Speziale, "On explicit algebraic stress models for complex turbulent flows", J. Fluid Mech. **254**, 59-78 (1993).
6. D. A. Johnson & L. S. King, "A mathematically simple turbulence closure model for attached and separated turbulent boundary layers", AIAA Journal, **23** (11), 1684-1692 (1985)
7. P. Bradshaw, D. H. Ferriss & N. P. Atwell, "Calculations of boundary-layer development using the turbulent energy equation", J. Fluid Mech. **28**, 593-616 (1967).
8. S. J. Kline, M. V. Cockrell, M. V. Morkovin & G. Sovan, eds. *Computation of Turbulent Boundary-Layers*, *Vol I*, AFOSR-IFP-Stanford Conference. (1968).
9. U. Schumann, "Realizability of Reynolds-stress models", Phys. Fluids **2**0, 721-725 (1977).
10. J. Wu, Y. Zhou & J. Wu, "Reduced stress tensor and dissipation and the transport of the Lamb vector", ICASE Report No 96-2, (1996)
11. H. Marmanis, "Analogy between the Navier-Stokes equations and Maxwell's equations: applications to turbulence", Phys. Fluids **10** (6), 1428-1437 (1998)
12. J. Kim, P. Moin & R. Moser, "Turbulence statistics in fully developed channel flow at low Reynolds number", J. Fluid Mech. **177**, 133-166 (1987).
13. P. A. Durbin, "On modeling three-dimensional turbulent wall layers", Phys. Fluids, **5** (5), 1231-1238 (1993).
14. P. Moin, T.-H. Shih, D. Driver & N. Mansour, "direct numerical simulation of a three-dimensional turbulent boundary layer", Phys. Fluids A, **2**, 1846-1853 (1990).